Microsc. Microanal. 13, 36–41, 2007
DOI: 10.1017/S1431927607070092

Microscopy AND Microanalysis

Detection of Filamentous Bulking Problems: Developing an Image Analysis System for Sludge Composition Monitoring

Rika Jenné, Ephraim Noble Banadda, Ilse Smets, Jeroen Deurinck, and Jan Van Impe*

BioTeC-Bioprocess Technology and Control, Katholieke Universiteit Leuven, Department of Chemical Engineering, W. de Croylaan 46, B-3001 Leuven, Belgium

Abstract: This article describes a fully automatic image analysis procedure for fast and reliable characterization of the activated sludge composition, that is, the floc and filament features. The algorithms developed for each of the analysis steps, that is, segmentation, object recognition, and characterization, are described in detail. Although the application range of the recognition method is *a priori* expanded by introducing a number of control parameters, the procedure proves to be intrinsically robust as it produces satisfactory results for a fixed set of parameter values for a wide variety of image types.

Key words: activated sludge characterization, filamentous bulking, image analysis, settleability monitoring

Introduction

Since the emergence of activated sludge systems for biological waste water treatment, almost a century ago, *filamentous bulking* has been causing operational problems in plants all over the world. This sludge settling failure is characterized by an imbalance between floc-forming and filamentous bacteria in the microbial aggregates of the sludge. With the effluent norms becoming stricter and stricter, the importance of computer-aided monitoring, control, and optimization of activated sludge plants is increasingly being recognized. Motivated by the success of image analysis in other domains, this research explores the potential of applying this novel technique to microscopic images of the activated sludge biomass, in the context of monitoring and detection of settling failures, like filamentous bulking.

Materials and Methods

Image Capturing and Analysis Equipment

Activated sludge images were captured manually using a light microscope with a total magnification of 100 times (Olympus BX 51), equipped with a 3CCD color video camera (Sony DXC-950P). Phase contrast illumination was applied to enhance the image contrast between the transparent, unstained biomass and the surrounding water. Microscopic images were digitized and stored as JPG (768 × 576 pixels) using Zeiss KS100.3 acquisition software. These images were subsequently processed and analyzed by means of the MATLAB *Image Processing Toolbox* 3.1 (The Mathworks, Inc., Natick, MA). With respect to the selected image type and pixel resolution, tests have shown that the analysis results when adopting another image type (e.g., BMP) or a higher pixel resolution are highly comparable while the processing time of the images and the required storage capacity increases substantially.

Received March 10, 2006; accepted October 8, 2006.
**Corresponding author*. E-mail: jan.vanimpe@cit.kuleuven.be

Results and Discussion

Image Segmentation

Phase contrast illumination produces images with bright flocs and dark filaments. Consequently, a specific segmentation approach is required. As double thresholding methods are not entirely satisfactory (Cenens et al., 2002), a single thresholding procedure was developed. In this approach, the original image is processed so that both flocs and filaments become visible in the same intensity region, and only one threshold is needed to separate them both from the background.

Glasbey and Horgan (1995) noted that a *top-hat transform* is suited for extracting small or narrow, bright or dark features in the image. Moreover, they mention that the transform can be used when variations in the background can prevent this from being achieved by simple thresholding. This transform is performed by subtracting the result from gray-scale closing from the original gray-scale image.

Table 1. Optimal Values for the Object Recognition Parameters

Parameter	Value		Units
	Red	*Blue*	
U	9 (×9)	13 (×13)	pixels
Q	0.025	0.015	—
W	15		%
V_1	1.1		—
V_2	1.3		—
T	5000		pixels
P	0.012		%

When applying this transform to an activated sludge image, followed by a rescaling, only two intensity fractions remain, that is, the (bright) background and the (dark) flocs and filaments. Note that an exponential rescaling (according to equation (1)) is required to return the pixel values to the range of 0 to 255 and to increase the contrast between background and objects. Thereafter, the image can be segmented with a single threshold, automatically determined using the *intermeans* algorithm (Glasbey & Horgan, 1995):

$$f_{ij,r} = \frac{255}{\exp(Q(f_{\max,s} - f_{\min,s})) - 1} \times [\exp(Q(f_{ij,s} - f_{\min,s})) - 1], \quad (1)$$

with $f_{ij,r}$ being the pixel value at position (i, j) in the rescaled image, $f_{ij,s}$ the pixel value at position (i, j) in the subtracted image, and $f_{\max,s}$ and $f_{\min,s}$ the highest and lowest pixel values, respectively, in the subtracted image.

To guarantee the flexibility of the segmentation procedure, two control parameters are integrated: the size of the structuring element for closing (*parameter U*) (Russ, 1995), which controls the spreading of intensities in the resulting image, and the exponential rescaling factor (*parameter Q*). In addition, it was found that the best results are obtained by applying this segmentation procedure to both the red and the blue parts of the color image, after which their respective binary images can be combined into the final segmentation result. The parameters U and Q are optimized individually for both color parts of the image, and the resulting values are listed in Table 1. A flowchart of the complete segmentation procedure is presented in Figure 1 (left) in which the OR box indicates a binary operation where a pixel is black if either one of the two images has a black pixel in that location of the image. Furthermore, small holes (with more than a fixed number of pixels) are filled to increase the continuity of the floc. This final image is then the starting point of the object recognition procedure as described below.

Object Recognition

The next critical step in the analysis of an activated sludge image is making the distinction between different object types, in this case flocs, filaments, and fragments. The problem of automatic floc and filament recognition in an activated sludge image was first addressed only very recently (Alves et al., 2000). In this work, an alternative approach was opted for, to take advantage of the specific characteristics of a phase contrast image. It was found that effective object recognition calls for a combination of three criteria, namely, based on brightness, shape, and size. How these criteria have been combined into an automatic recognition procedure for flocs, filaments, and fragments is illustrated by the flowchart in Figure 1 (right).

Shape

The most frequently used shape parameters are made up of a combination of different size descriptors (Russ, 1995). Seeing that flocs are more circular with an irregular border, whereas filaments are more elongated and smooth, four shape parameters have been tested to make this distinction: the aspect ratio (*AR*), the roundness (*R*), the form factor (*FF*), and the reduced radius of gyration (*RG*). The last mentioned was found to produce the largest percentage of correct classifications of flocs and filaments (Jenné et al., 2002). The optimal threshold value of *RG* equal to 1.1 comes close to that used by da Motta et al. (2001) (i.e., $RG = 1$) and Dagot et al. (2001) (i.e., $RG = 0.9$). Therefore, the value of the reduced radius of gyration of each object (*RG*) forms a first control parameter (*parameter V*) in the object recognition procedure. Note that this criterion is applied twice during the procedure, once to separate flocs from free filaments (Criterion IIa in Fig. 1), and a second time to rejoin dark pixel groups with flocs that were mistaken for filaments (Criterion IIb in Fig. 1). Also note that the criteria as mentioned in this text are expressed in terms of floc recognition, meaning for this criterion that the object is (probably) a floc if its RG value is smaller than parameter *V*:

$$\text{Criterion} = RG < \textit{parameter V}.$$

Brightness

Because the above shape criterion only separates flocs from *free* filaments, that is, filaments not in contact with flocs, a second criterion is necessary to *disconnect* any filament attached to one or more flocs. In phase contrast images, flocs are lighter than the background, whereas filaments are darker. A brightness criterion can thus be defined in which the brightness (value) of the object pixels (f_{ij}) is compared to an intensity threshold (I_R). This intensity value is automatically adjusted for each image, based on the pixel count in the image histogram. An intensity I_T is determined as the pixel value at which the number of pixels is larger and closest to a prespecified amount (controlled by *param-*

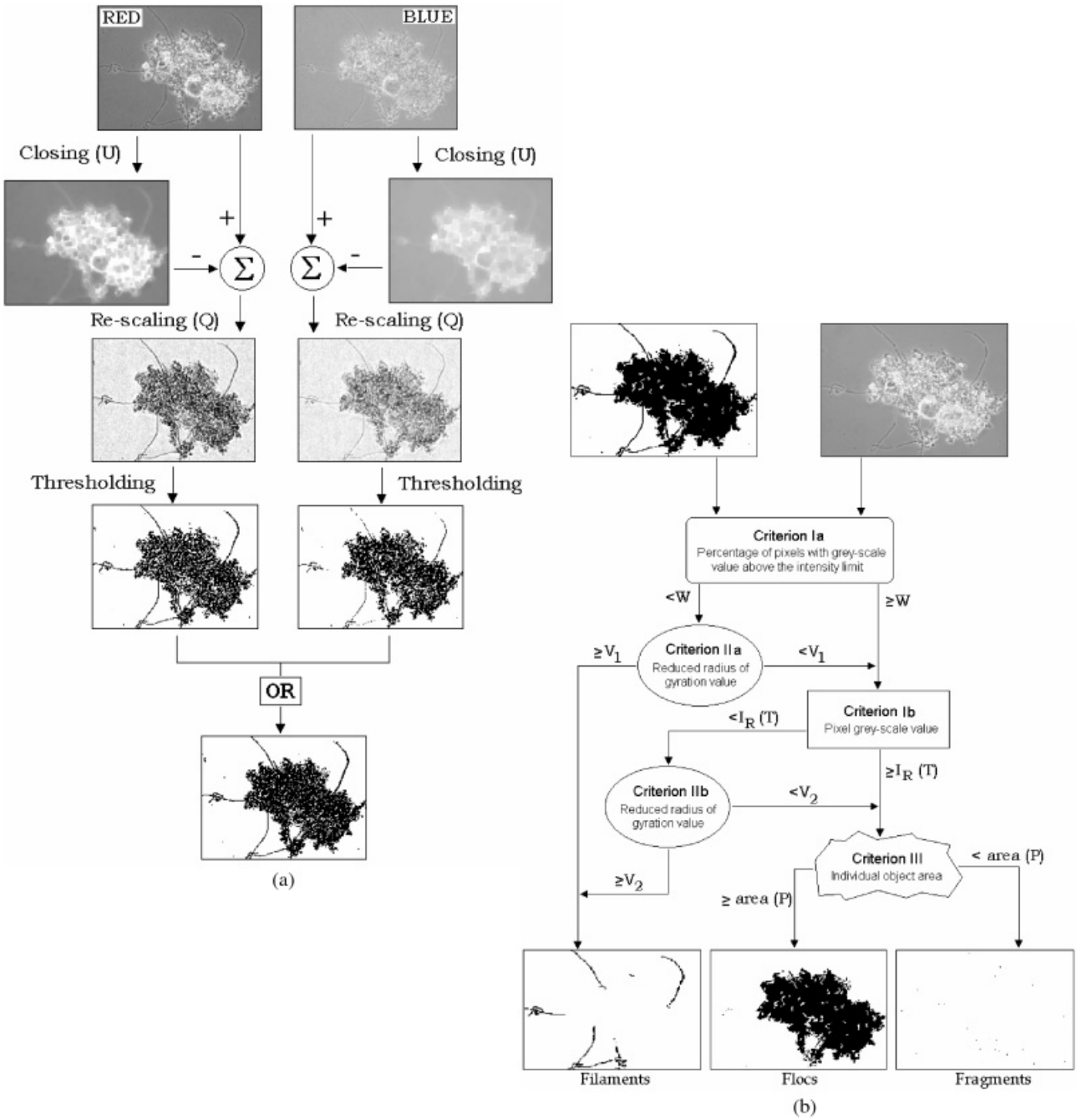

Figure 1. a: Program flowchart of the segmentation procedure. **b:** Program flowchart of the object recognition procedure.

eter T). Thereafter the intensity reference is set equal to the corresponding value on the other side of the histogram peak as follows: $I_R = I_{max} + (I_{max} - I_T)$ (see Fig. 2 and Criterion Ib in Fig. 1):

$$\text{Criterion} = f_{ij} \geq I_R \,(\textit{parameter } T).$$

In analogy with the shape criterion, the brightness of the total object can also be used to separate flocs from *free* filaments. In that case, the criterion is adjusted to evaluate the percentage of object pixels with a value above the intensity threshold (I_R). This percentage of object pixels is controlled by *parameter W* (Criterion Ia in Fig. 1):

$$\text{Criterion} = \{\#\, f_{ij} \geq I_R \,(\textit{parameter } T)\}$$

$$\geq \textit{parameter } W \times \textit{object area}.$$

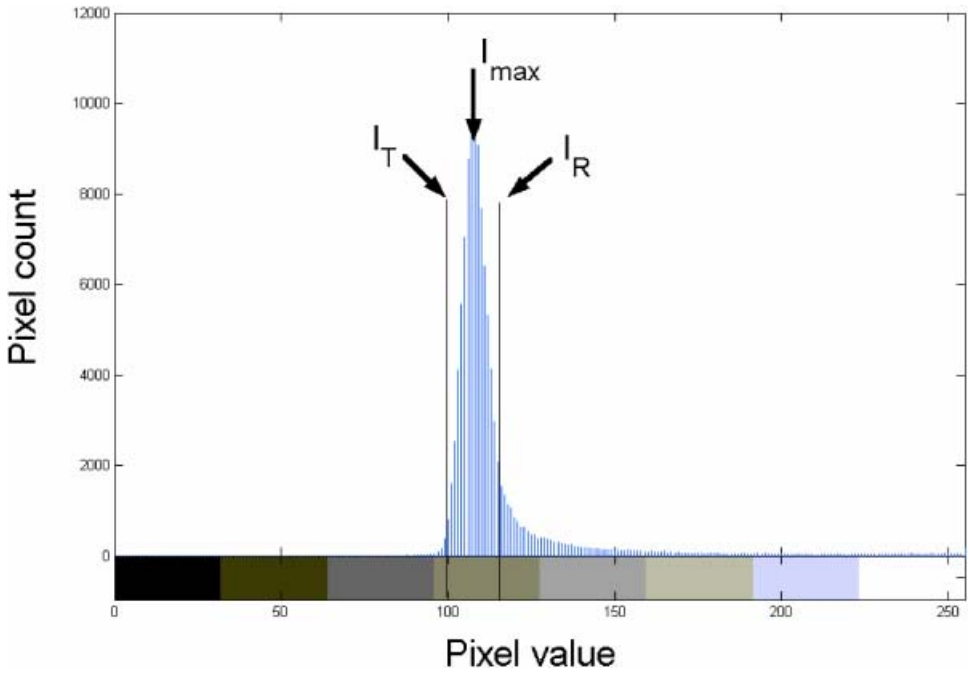

Figure 2. Determination of the intensity reference for brightness evaluation, based on the gray-scale histogram of the image background.

Note that criteria Ia and IIa are complementary, and that the order of application does not significantly affect the result. The combination of these two criteria always results in a group of filaments on the one hand and a group of flocs on the other hand, some of which still have filaments attached to their border.

Size

After separating the objects into flocs and filaments, the floc category still contains some debris, that is, dispersed bacteria, tiny flocs, and filaments or organic and inorganic waste material. These *fragments* can be separated from the flocs based on their individual projected areas, more specifically the percentage of object pixels of the total image. The size criterion brings about a final control *parameter P*, that is, a fixed percentage of the image area:

$$\text{Criterion} = \textit{object area} \geq \textit{parameter } P \times \textit{image area}.$$

Figure 3 depicts the results of this automatic object recognition method for three images of various origins, as well as their respective original gray-scale images. These images are processed with the same values for each of the five recognition parameters; the values are listed in Table 1. Hence, the same remark applies for this stage of the procedure as for the segmentation step: Although the application range of the recognition method is *a priori* expanded by introducing a number of control parameters, the procedure is intrinsically robust as it produces satisfactory results for a fixed set of parameter values for a wide variety of image types.

Quantification and Characterization

Problems with filament counting and characterization are anticipated, as object labeling generates filament clusters rather than individual filaments. Consequently, the program will have to stick to global filament measurements, that is, the total filament length per image (F). For fragments, the same holds true, as they are too small for accurate individual measuring. Therefore, the individual object characterization focuses on flocs. On the one hand, floc size can be expressed, as the appropriate algorithms for area, perimeter, length, and breadth estimation have been implemented. On the other hand, justification of the implemented set of floc shape measurements is found in literature references and amounts to seven dimensionless descriptors (Grijspeerdt & Verstraete, 1996, 1997; da Motta et al., 2001; Heine et al., 2002; Govoreanu et al., 2003). The aspect ratio (AR), the roundness (R), and the reduced radius of gyration (RG) are expected to exhibit a sensitivity to elongation, whereas the form factor (FF) and the fractal dimension (FD) are thought to be affected by boundary roughness; the values of solidity (S) and convexity (C) will depend on how convex the object is. The definitions of AR, R, FF, RG, C, and S are given in equations (2)–(8). FD is computed by means of the box-counting algorithm (Klonowski, 2000).

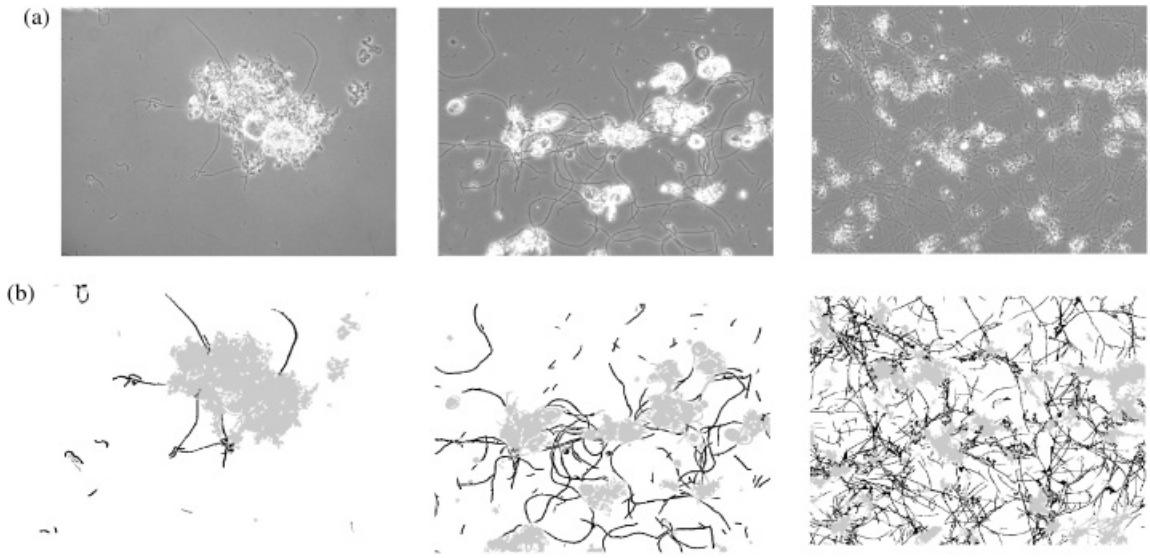

Figure 3. a: Activated sludge images of different origin and captured with different equipment. Left: Image of *domestic* activated sludge, captured with a Zeiss Axiostar microscope and a Sony DXC-950P camera. Middle: Image of *brewery* activated sludge, captured with a Leica DMLB microscope and a Leica DC200 camera. Right: Image of bulking sludge (laboratory induced), captured with an Olympus BX51 microscope and a Sony DXC-950P camera. **b:** Results of automatic segmentation and object recognition according to the procedures depicted in Figure 1.

$$D_{eq} = 2\sqrt{\frac{area}{\pi}}, \tag{2}$$

$$R = \frac{4}{\pi}\frac{area}{length^2}, \tag{3}$$

$$RG = \frac{\sqrt{M_{2x} + M_{2y}}}{D_{eq}/2}, \tag{4}$$

where M_{2x} and M_{2y} are second order moments,

$$AR = \frac{length}{breadth}, \tag{5}$$

$$FF = 4\pi\frac{area}{perimeter^2}, \tag{6}$$

$$C = \frac{perimeter_{convex}}{perimeter}, \tag{7}$$

and

$$S = \frac{area}{area_{convex}}. \tag{8}$$

Procedure Evaluation: Laboratory-Scale Experiments

To assess the image analysis methodology in a practical situation, experiments were performed in a controlled laboratory-scale activated sludge system with a classic configuration. By applying specific process condition, that is, increased sludge loading, filamentous bulking events were successfully induced in three long-term monitoring periods (Jenné et al., 2004). Correlations between image information and sludge settleability were sought and consistent trends were identified, relating the sludge settleability (in terms of sludge volume index, SVI) to the image characteristics of flocs and filaments described above. More specifically, at the onset of a filamentous bulking problem, that is, an increase in sludge volume index, the image analysis procedure records an increase in filament abundance as well as changes in floc shape, the overall floc structure becoming more elongated and more diffuse. It is suggested that the changes in floc shape can be mainly attributed to changes in filament abundance, as explained by the filamentous backbone theory. This implies that changing process conditions may have an indirect rather than a direct effect on the morphology of activated sludge flocs.

Conclusion

In this article, a fully automatic procedure for activated sludge image analysis is presented. The accurate and objec-

tive, yet fast and practical approach makes the developed image analysis procedure suitable for integration into an online sensor for monitoring settling properties in full-scale activated sludge systems. Ongoing research includes testing the procedure on a variety of full-scale installations.

Acknowledgments

Work supported by projects OT/03/30 of the KULeuven Research Council, and the Belgian Program on Interuniversity Poles of Attraction, initiated by the Belgian Federal Science Policy Office. R. Jenné is a postdoctoral fellow with the KULeuven Research Council (PDM/04/150/BM). I.Y. Smets is a postdoctoral fellow with the Fund for Scientific Research Flanders (FWO-Vlaanderen). The scientific responsibility is assumed by its authors.

References

Alves, M., Cavaleiro, A.J., Ferreira, E.C., Amaral, A.L., Mota, M., da Motta, M., Vivier, H. & Pons, M.-N. (2000). Characterisation by image analysis of anaerobic sludge under shock conditions. *Water Sci Technol* **41**, 207–214.

Cenens, C., Van Beurden, K.P., Jenné, R. & Van Impe, J.F. (2002). On the development of a novel image analysis technique to distinguish between flocs and filaments in activated sludge images. *Water Sci Technol* **46**, 381–387.

Dagot, C., Pons, M.N., Casellas, M., Guibaud, G., Dollet, P. & Baudu, M. (2001). Use of image analysis and rheological studies for the control of settleability of filamentous bacteria: Application in SBR reactor. *Water Sci Technol* **43**, 27–33.

Da Motta, M., Pons, M.N. & Roche, N. (2001). Automated monitoring of activated sludge in a pilot plant using image analysis. *Water Sci Technol* **43**, 91–96.

Glasbey, C.A. & Horgan, G.W. (1995). *Image Analysis for the Biological Sciences*. New York: John Wiley & Sons.

Govoreanu, R., Seghers, D., Nopens, I., De Clercq, B., Saveyn, H., Capalozza, C., Van der Meeren, P., Verstraete, W., Top, E. & Vanrolleghem, P.A. (2003). Linking floc structure and settling properties to activated sludge population dynamics in an SBR. *Water Sci Technol* **47**, 9–18.

Grijspeerdt, K. & Verstraete, W. (1996). A sensor for the secondary clarifier based on image analysis. *Water Sci Technol* **33**, 61–70.

Grijspeerdt, K. & Verstraete, W. (1997). Image analysis to estimate the settleability and concentration of activated sludge. *Water Res* **31**, 1126–1133.

Heine, W., Sekoulov, I., Burkhardt, H., Bergen, L. & Behrendt, J. (2002). Early warning-system for operation failures in biological stages of WWTPS by on-line image analysis. *Water Sci Technol* **46**, 117–124.

Jenné, R., Banadda, E.N., Smets, I.Y., Gins, G., Mys, M. & Van Impe, J.F. (2004). Developing an early warning tool for filamentous bulking problems based on image analysis. In *Proceedings of the Second International IWA Conference on Automation in Water Quality Monitoring, AutMoNet 2004*, Vienna, Austria, Langergraber, G., Winkler, S., Fleischmann, N., Pressl, A. & Haberl, R. (Eds.), pp. 221–228.

Jenné, R., Cenens, C., Geeraerd, A.H. & Van Impe, J.F. (2002). Towards on-line quantification of flocs and filaments by image analysis. *Biotechnol Lett* **24**, 931–935.

Klonowski, W. (2000). Signal and image analysis using chaos theory and fractal geometry. *Mach Graph Vision* **9**, 403–431.

Russ, J.C. (1995). *The Image Processing Handbook*. 3rd ed. Boca Raton, FL: CRC Press.